D38 Is an Essential Part of the Proton Translocation Pathway in Bacteriorhodopsin†

Jens Riesle,‡ Dieter Oesterhelt,‡ Norbert A. Dencher,§ and Joachim Heberle*,‖

Max-Planck-Institut für Biochemie, 82152 Martinsried, Germany, Technische Hochschule Darmstadt, Institut für Biochemie, 64287 Darmstadt, Germany, and Forschungszentrum Jülich GmbH (KFA), IBI-2, 52425 Jülich, Germany

Received January 9, 1996; Revised Manuscript Received March 18, 1996⊗

ABSTRACT: At present, almost no knowledge exists about the functional relevance of the amino acid residues at the cytoplasmic (CP) surface of the light-driven proton pump bacteriorhodopsin (BR) although a prerequisite for efficient vectorial proton translocation is the efficient capture of protons from the alkaline cytoplasm of the cell. To identify residues involved in the proton transfer reaction steps in the CP part of BR, the aspartic and glutamic amino acids D36, D38, D102, D104, and E161 were replaced by cysteine and arginine (i.e., a negatively charged residue by a neutral or positive one at the pH of investigation). The effect of these replacements on the photo- and transport cycle was examined by time-resolved visible and infrared spectroscopy, biochemical modification studies, and activity assays in intact cells. Of the five CP amino acids studied, only the replacement of D38 resulted in severe alterations of the reaction steps in BR during the second half of the photocycle. Our data show that D38, which seemed to be a freely accessible CP surface residue lacking functional importance, is an essential part of the CP proton uptake pathway connecting the membrane surface with the Schiff base of BR, probably as the first amino acid residue at the CP entrance. D38 influences the late steps in the functional cycle, such as the occurrence of the intermediates N and O, the modulation of the hydrogen-network, the conformational changes in the protein moiety, and the deprotonation/reprotonation of D96. Opposed to this function, the surface-exposed amino acids D36, D102, D104, and E161 seem to efficiently collect protons from the aqueous bulk phase and funnel them to the entrance of the CP proton pathway.

Proton transport is an essential step in energy transduction (Mitchell, 1961; Boyer, 1977). The light-driven proton pump bacteriorhodopsin (BR)[1] translocates a proton from the inside of the cell to the external medium, thereby establishing a proton gradient across the plasma membrane and allowing the halobacterial cell to use sunlight as its only energy source (Oesterhelt et al., 1992).

BR is the only protein found in the purple membrane, a two-dimensional crystalline lattice in the plasma membrane of *Halobacterium salinarium* (Oesterhelt & Stoeckenius, 1971; Blaurock & Stoeckenius, 1971). Mainly four of the seven transmembrane helices (B, C, F, and G) form a transmembrane proton channel (Figure 1A). The chromophore retinal, bound to Lys216 via a protonated Schiff base, is located approximately in the middle of BR, thereby preventing the free diffusion of protons (Burghaus & Dencher, 1989) and separating an extracellular (EC) from a cytoplasmic (CP) channel (Figure 1B). Upon photon absorption, retinal isomerizes around the C13−C14 bond and thermally reverts to the initial *all-trans* state, thereby passing a series of photocycle intermediates termed J, K, L, M, N, and O [see recent review by Lanyi (1993)]. The photocycle is tightly coupled to proton transport. During the L → M step, D85 is protonated by the Schiff base (Braiman et al., 1988), and a proton is released to the EC membrane surface (Heberle & Dencher, 1990, 1992a,b), followed by reprotonation of the Schiff base from D96 (M → N) (Butt et al., 1989; Otto et al., 1989; Gerwert et al., 1990) and subsequent proton uptake from the cytoplasm/reprotonation of D96 (during N → O at physiological pH; Cao et al., 1993).

Recently, we have analyzed the pathway of the protons released to the extracellular surface of BR using the planar PM as an open membrane system (Heberle et al., 1994). With the help of covalently bound pH indicators, we found that protons move long distances along the membrane surface (lateral proton transfer) before they equilibrate with the aqueous bulk phase. These findings were confirmed by Alexiev et al. (1995).

In the current study, we focus on the functional role of CP surface amino acids on the proton uptake by BR (reprotonation of D96 from the bulk) and the decay of the photocycle intermediate M (reprotonation of the Schiff base from D96), i.e., on the second half of the BR photocycle.

At present, there is almost no knowledge about the functional relevance of the residues at the CP surface, and the existing reports are contradictory. It was reported that the mutants D36N, D38N, D102N, and D104N, as expressed in *E. coli*, have a slightly decreased M-decay time (Stern et al., 1989), but the same or a higher proton pumping rate as the wild type (Mogi et al., 1988). Stern et al. concluded

†This work was supported by the Deutsche Forschungsgemeinschaft (SFB 189/B15 to J.H. and SFB 312/B4 to N.A.D.) and the Fonds der Chemischen Industrie (to N.A.D.). J.R. was partly supported by the Stiftung-Stipendien-Fonds des Verbandes der Chemischen Industrie in terms of a Kekulé fellowship.

* Author to whom correspondence should be addressed. Fax: 49-2461-612020.

‡ Max-Planck-Institut für Biochemie.

§ Institut für Biochemie.

‖ Forschungszentrum Jülich GmbH (KFA).

⊗ Abstract published in *Advance ACS Abstracts,* May 1, 1996.

[1] Abbreviations: BR, bacteriorhodopsin; D36C and other mutant proteins, bacteriorhodopsin with aspartic acid 36 replaced by cysteine (double mutant $D_2102,104R_2$, aspartic acid 102 and 104 replaced by arginine); CP, cytoplasmic; EC, extracellular; FMI, fluorescein-5-maleimide; FT-IR, Fourier transform infrared; DTT, 1,4-dithio-DL-threitol; EDTA, ethylenediaminetetraacetic acid; DMSM, 2,5-dimethoxystilbene-4′-maleimide; CPM, 7-(diethylamino)-3-(4′-maleimidophenyl)-4-methylcoumarin; DMF, dimethylformamide.

S0006-2960(96)00045-1 CCC: $12.00

that these residues do not have an important role in the photocycle or in the proton pumping mechanism. At this point, it should be stressed that for a number of mutants, as well as for wild type, considerable differences in the phenotypes have been observed when the protein was expressed in *H. salinarium* or in *E. coli* (Lanyi, 1993; Heberle et al., 1993). In the present study, homologously expressed mutant BR is studied in its natural PM lattice. Therefore, changes in the kinetics of the photocycle and the pumping cycle can solely be attributed to functional differences in the exchanged amino acids.

Incubation of cation-depleted BR with Fe^{3+} and pentaamineaquocobalt(III) tetrafluoroborate led to a drastic retardation of the M decay (Engelhard et al., 1989, 1990). The data suggest that carboxyl groups on the CP surface of BR are involved in the interaction with these compounds, although the definite site of modification/interaction is unknown.

The prerequisite for efficient vectorial proton translocation by BR is the efficient capture of protons from the alkaline cytoplasm of the cell. Especially because of the fast transient protonation dynamics of carboxylic groups, the amino acids Asp and Glu might contribute to the collection of protons from the cell interior (Nachliel et al., 1996).

We report here on the effect on proton translocation steps in the CP part of BR by substitutions of the aspartic and glutamic acids D36, D38, D102, D104, and E161 with cysteine (p*K* 8.5) or arginine (p*K* 12.5) residues. According to the structure of BR as determined by Henderson et al. (1990), D38 might play a key role in these proton transfer steps because of its location at the entrance of the CP channel, although up to now it was considered as a surface-exposed residue without functional relevance (Stern et al., 1989). Indeed, we were able to show that D38 is in fact an essential part of the CP proton uptake pathway connecting the membrane surface with the Schiff base of BR, probably as the first amino acid residue at the CP entrance. Furthermore, D38 is involved in the initiation of important steps in the functional cycle. The surface-exposed amino acids D36, D102, D104, and E161 seem to be involved in the efficient collection of protons from the aqueous bulk phase and funnel them to D38.

MATERIALS AND METHODS

FMI, DMSM, and CPM were obtained from Molecular Probes. Pyranine (8-hydroxy-1,3,6-pyrenetrisulfonate) was purchased from Kodak. All other chemicals used were of analytical grade.

Mutagenesis and Expression. Site-specific mutants of bacteriorhodopsin, D36C, D38C, D38R, E161C, and D_2102,-$104R_2$, were prepared according to Ferrando et al. (1993). Mutagenesis was followed by transformation and homologous expression in *H. salinarium* strains HN5 (Rumpel and Oesterhelt, unpublished results) and L33 (Wagner et al., 1981) with the help of the shuttle plasmid pEF 191. Mutated proteins were isolated as purple membrane sheets according to Oesterhelt and Stoeckenius (1974). The mutations were confirmed from *H. salinarium* transformants by sequencing the PCR-amplified *bop* gene from isolated total DNA.

Modification of Cysteine in Mutant BR. Selective labeling of the cysteine mutants with fluorescein derivatives was performed as described in Heberle et al. (1994). A labeling stoichiometry of 0.7−1 fluorescein per BR was achieved. Qualitative accessibility assays were performed by incubating 1 nmol of the Cys mutant in 10 mL of 100 mM sodium phosphate, pH 7.0, 2 mM EDTA, with a 30-fold excess of the fluorescent maleimides DMSM or CPM (in DMF; final concentration below 5%) for 1 h at 37 °C or overnight at room temperature under an argon atmosphere. Analysis was carried out by excitation with UV light and comparison of the fluorescence intensity with that of a mercaptoethanol sample of the same thiol concentration. BR wild type served as a negative control.

Proton Translocation Activity of Mutant BR in H. salinarium Cells. Specific proton translocation was measured according to Oesterhelt (1982) at pH 7.0. Samples were thermostated at 20 °C. Illumination was from a 150 W halogene lamp (OG 515 filter, Schott), providing a light intensity of about 100 mW/cm^2 at the place of the sample. Light-saturating conditions were checked with a 50% transmission filter.

Flash Spectroscopy. Time-resolved visible absorption spectroscopy was performed as described by Heberle et al. (1993). PM (8−12 μM BR) was suspended in 150 mM KCl (pH 7.2). For the evaluation of proton transfer reactions with pyranine (40 μM, as pH indicator for the aqueous bulk phase), measurements of samples with l0 mM imidazole buffer, pH 7.2, were subtracted from measurements without buffer. Negative absorbance changes at 465 nm reflect protonation of the pH indicator. Samples were thermostated at 20 °C.

Time-Resolved FT-IR Difference Spectroscopy. Time-resolved FT-IR measurements were done on a Bruker IFS 66V spectrometer equipped with step-scan option. For pulsed excitation, a similar Nd:YAG-laser was used as for the time-resolved measurements in the visible (frequency-doubled output at 532 nm, pulse duration 8 ns, excitation energy 5 mJ pulse^{-1} cm^{-2}). Concentrated samples of mutated or wild-type BR (about 150 μg in 10 mM KCl and 1 mM potassium phosphate buffer, pH 7.2) were deposited on CaF_2 windows and slowly dried at room humidity. Samples were placed in a closed chamber and rehydrated overnight at 96% relative humidity (saturated KNO_3 solution). The OH-stretching band around 3400 cm^{-1} served as qualitative measure for the water content of the samples. At 1658 cm^{-1}, where the overlap of water and amide I bands is at maximum, the band height exceeded that of the amide II band (1546 cm^{-1}) by a factor of about 1.3. This, and the fact that the kinetics of the C═C stretching vibration (1527 cm^{-1}) and the electronic ground-state depletion signal (570 nm) are identical, ensures that the hydrated samples used for FT-IR and the purple membrane suspensions for visible absorption spectroscopy are identical in the kinetics of their photoinduced reactions. The time resolution of the FT-IR step-scan measurements is currently limited by the analog digital converter to 5 μs. A broad band interference filter limited the free spectral range from 1900 to 1000 cm^{-1}. At 4.5 cm^{-1} spectral resolution, 20 measurements at each mirror position were co-added. The repetition frequency of the excitation laser was 3 Hz at maximum, depending on the photocycle kinetics. Thus, complete recording of a step-scan measurement took usually not more than 1.5 h without harming the sample. Interferograms were apodized with a Blackman−Harris 3-term function and zero-filled with a

factor of 2. Resulting data were further processed by co-adding difference specta on a logarithmic time scale. For lower time resolution, the rapid-scan technique was applied, and a complete spectrum could be recorded within 14 ms. Samples were thermostated at 20 °C. A complete description of the FT-IR setup is presented elsewhere (Heberle & Zscherp, 1996).

RESULTS

As indicated in Figure 1, the aspartic and glutamic acids (p*K* 3.7 and 4.1, respectively, for isolated amino acids in aqueous environment) that were mutated are located at helix B (D38) and the cytoplasmic loops A−B (D36), C−D (D102, D104), and E−F (E161) of BR. Negatively charged amino acids (D, E) were replaced by residues either neutral (C, p*K* = 8.5) or positively charged (R, p*K* = 12.5) at pH 7. Because the mutated amino acids are on the surface of BR, no structural perturbation of the protein is expected. The visible absorbance maxima of the mutants were identical to that of the wild type as were the absorbance shifts upon light−dark adaptation and retinal isomer composition (data not shown). Also, vibrational bands of BR and the mutants appear at the same wavenumber (see below). This indicates that no structural changes influencing the chromophore binding pocket are induced by the mutations.

Accessibility of the Cysteine Residue in Mutant BR. The cysteine mutants were incubated with the maleimide dyes FMI, DMSM, and CPM (with differing size and hydrophobic character), in order to analyze the accessibility of the SH groups in positions 36, 38, and 161. Two of them (DMSM, CPM) are actually nonfluorescent until they react with a thiol, making them well suited for a qualitative accessibility assay. Under the labeling conditions applied, amino acid residues C36 and C161 in the mutant BRs are accessible for all maleimide dyes, but C38 only for FMI, suggesting a more buried position of D38 in the protein.

Proton Transport Activity of Mutant BR in H. salinarium Cells. Stern et al. (1989) reported that the mutants D36N, D38N, D102N, and D104N, expressed in *E. coli*, have a slightly decreased M decay time, but the same or a higher proton pumping rate compared to wild type (Mogi et al., 1988). In contrast, we found that the retardation of the rate-limiting M decay in the mutant BRs reported here (measured in 150 mM KCl) correlates with the specific proton transport activities in *H. salinarium* cells. The initial rate of pH decrease upon illumination was measured under light saturating conditions. Wild-type BR has a turnover of 250 protons per BR per minute. The proton translocation activity of the mutant D38C was 55% of the wild type, 41% for D_2102,-$104R_2$, and 30% for D38R. Although not quantitatively, the order of retardation in M decay and pyranine deprotonation therefore corresponds to the decrease in turnover under *in vivo* conditions. Thus, the presence of the negatively charged amino acids at the cytoplasmic side is relevant for the activity of BR in intact cells.

Effect of Mutations on M Decay and Proton Uptake Kinetics. In this study, we focus on the proton uptake by BR (deprotonation of the pH sensitive dye pyranine, indicating reprotonation of the protein surface residues from the bulk) and the decay of the photocycle intermediate M (reprotonation of the Schiff base from D96), i.e., the second half of the BR photocycle.

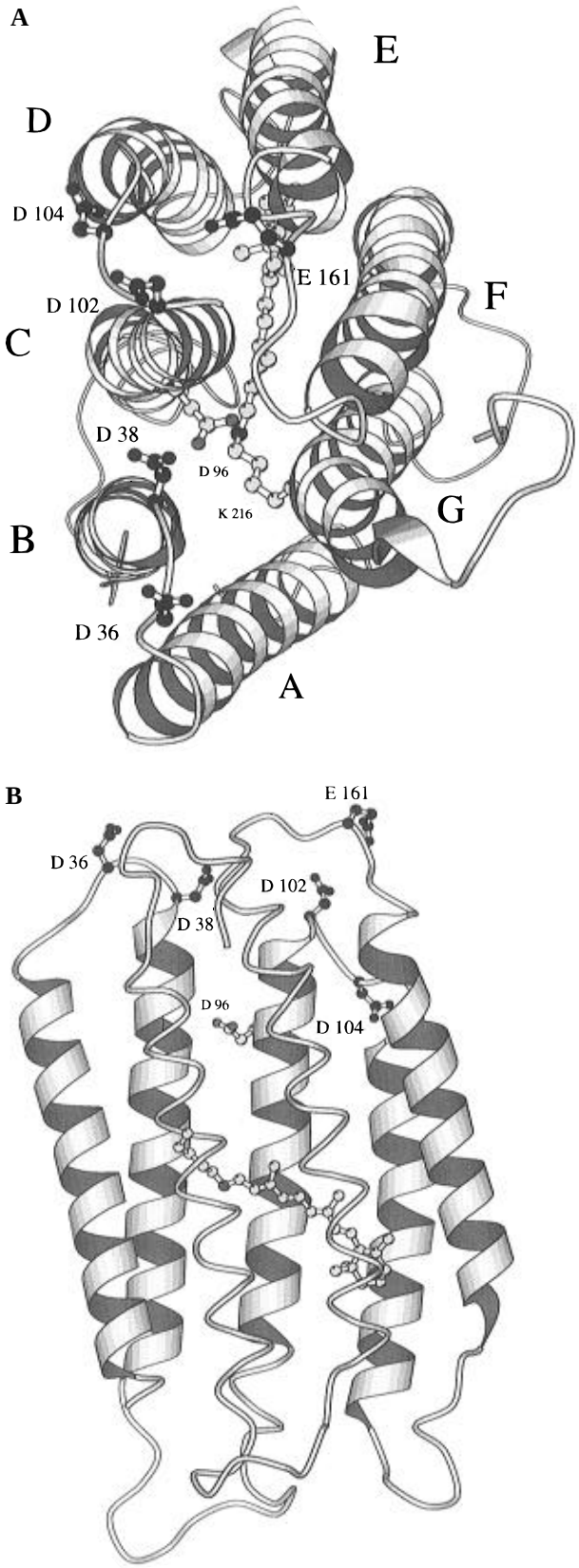

FIGURE 1: Ribbon representation of BR according to Nonella and Oesterhelt (unpublished results), including the chromophore retinal, K216, D96, and the mutated amino acids on the cytoplasmic surface, generated with MOLSCRIPT (Kraulis, 1991). (A) Top view on the cytoplasmic surface of BR. (B) Side view of the protein; helices F and G are shown as lines to reveal the protein interior.

In Figure 2, the kinetics of M (upper traces) of wild type, D36C, and E161C are compared with the pH changes detected by the highly water-soluble pyranine (P) in the

Table 1: Time Constants and Amplitudes (Below) Resulting from Multiexponential Fitting to the Data Traces Depicted in Figures 2 and 3[a]

	components of M kinetics						mono M	pyranine	
sample	1	2	3	4	5	6	decay	H^+ release from BR	H^+ uptake by BR
wild-type	1.0 μs	55 μs	182 μs	1.8 ms	5.3 ms	10 ms	6 ms	824 μs	12 ms
	−12%	−31%	−57%	9%	71%	20%	100%	100%	−100%
E161C	1.3 μs	50 μs	179 μs	2.3 ms	9.9 ms	58 ms	7.3 ms	1.2 ms	25 ms
	−13%	−36%	−51%	48%	45%	7%	100%	100%	−100%
D36C	2.2 μs	65 μs	175 μs	2.3 ms	11 ms	53 ms	8.8 ms	1.5 ms	19 ms
	−12%	−36%	−52%	31%	62%	7%	100%	100%	−100%
D38C	0.5 μs	47 μs	161 μs	11 ms	28 ms		23 ms	832 μs	23 ms
	−12%	−26%	−62%	26%	74%		100%	100%	−100%
$D_2$102,104R_2	1.5 μs	93 μs	279 μs	19 ms	46 ms		38 ms	1.6 ms	49 ms
	−7%	−77%	−16%	25%	75%		100%	100%	−100%
D38R	1.6 μs	95 μs	279 μs	57 ms	91 ms		87 ms	702 μs	88 ms
	−10%	−59%	−31%	16%	84%		100%	100%	−100%

[a] Negative amplitudes of exponentials correspond to a transient rise in absorbance. For convenience, the results of a monoexponential fitting of the M decay are also listed. Protonation of pyranine, denoted as H^+ release from BR, reflects the proton transfer kinetics from the membrane surface into the aqueous bulk.

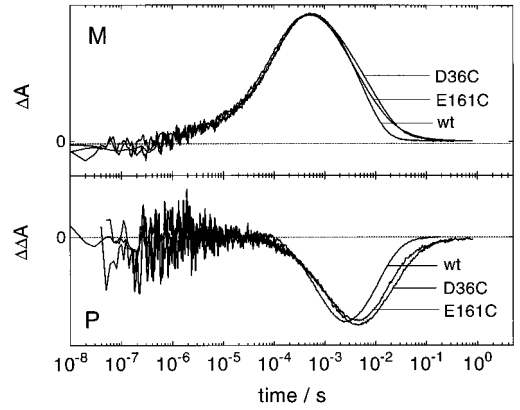

FIGURE 2: (M) Kinetics of M formation and decay (measured at 412 nm) for wild-type BR (wt) and the Cys mutants D36C and E161C. (P) Transient pH changes in the aqueous medium detected by pyranine (at 465 nm) for wild-type BR and mutants. Measurements were at pH 7.2, 20 °C, and in 150 mM KCl.

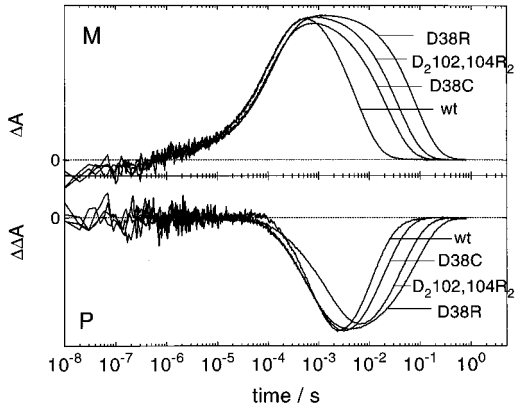

FIGURE 3: M kinetics (M) and corresponding pH changes in the aqueous phase (P) for different mutations at the cytoplasmic surface of BR (point mutants D38C and D38R and the double mutant D_2-102,104R_2). For comparison, wild-type kinetics are also depicted (wt).

aqueous bulk phase (lower traces) following excitation with a laser flash. Light-induced ejection of the protons to the EC side of BR, which can only be time-resolved-detected by surface-bound pH probes, occurs in about 70 μs. The delayed transfer of the released protons from the membrane surface to the bulk is monitored by pyranine with a decrease in absorbance (protonation of P) (Heberle & Dencher, 1992a). Proton transfer from the bulk to the CP surface of BR is detected by the absorbance increase of pyranine to the initial value (deprotonation of P). The same kinetics of proton uptake are measured by a pH indicating dye covalently bound to the CP surface (Heberle et al., 1994). As depicted in Figure 2, a slightly retarded M decay as well as a slower deprotonation of pyranine was observed for both the D36C and E161C mutants relative to the wild-type. On the other hand, the M rise time of mutant BRs is within experimental error the same as in the wild type (Table 1).

Figure 3 compares the mutants D38C, $D_2$102,104R_2, and D38R with the wild type. Retardation of M decay and of deprotonation of pyranine is more pronounced in $D_2$102,-104R_2 and D38R (Figure 3) than in D36C and E161C. In particular, the M decay is influenced more strongly by the cysteine substitution in position 38 than in 36. Furthermore, D38R shows a stronger retardation than $D_2$102,104R_2, although two aspartates have been exchanged for arginines in the latter case (charge change +2 versus +4, respectively). From all replacements carried out, the strongest effect is seen in mutation D38R, which comes close to the range of time constants for D96 mutants (Tittor et al., 1989; Miller & Oesterhelt, 1990). M decay of D38C, $D_2$102,104R_2, and D38R is described by only two exponentials, whereas wild type, E161C, and D36C are satisfactorily fitted by three exponentials (Table 1). To get a rough estimate of the overall M decay time, a single exponential fit has also been applied (column mono M decay in Table 1).

Bulk/surface transfer is slower by a factor of 2 in wild type than proton transfer to the Schiff base during M decay (see Table 1). For the mutant proteins with a decreased negative cytoplasmic surface charge, a slower proton uptake from the bulk relative to the wild type is expected. If this were be true, however, the M decay reflecting the kinetics of the intramembrane proton transfer should be unchanged in the mutants, as found for E161C and D36C. In contrast, a decrease of this rate, correlating well with the rate of pyranine deprotonation, is found for mutants D38C, D38R, and $D_2$102,104R_2 (Table 1). This is not expected because the reprotonation of the Schiff base via the proton donor D96 should not be influenced by the surfaces residues. Therefore, the rate of Schiff base reprotonation (M decay) should be as in wild type. Because it is not, we have to assume that additional residues, especially the residue in

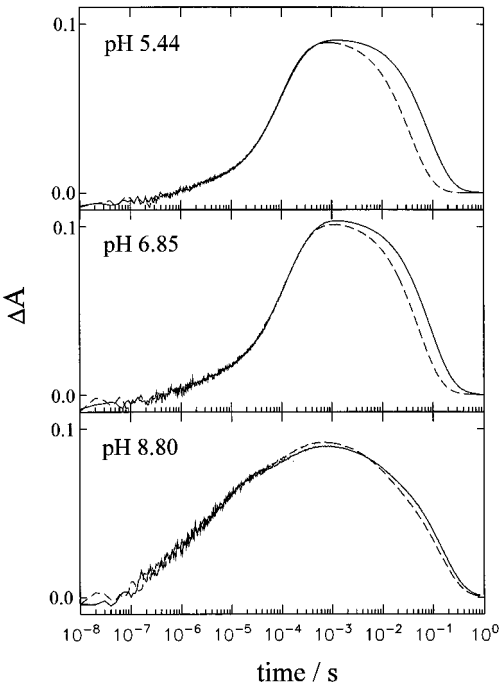

FIGURE 4: Influence of azide (0.5 M, dashed line) on the kinetics of the M intermediate of the D38R mutant monitored at three different pH values (5.44, 6.85, and 8.80).

position 38, determine the rate of reprotonation of the Schiff base.

Effect of Azide on M Decay. Azide accelerates the retarded M decay of some BR mutants back to wild-type values or even stronger (Tittor et al., 1989). Proton conduction in the cytoplasmic half-channel of BR D96N mutant limiting M decay is accelerated by more than 100-fold after addition of azide (Tittor et al., 1989). The mechanism of azide action in D96 mutants was investigated by FT-IR (le Coutre et al., 1995), and azide was suggested to restore efficient proton conduction in the hydrogen-bonded network of the proton uptake pathway which is kinetically impaired by the lack of D96. Therefore, it was of interest to investigate the effect of azide on the surface mutant BRs.

For example, in Figure 4, M kinetics of mutant D38R with (0.5 M, dashed line) and without azide (continuous line) are compared at different pH values. The M decay of D38R is very little dependent on pH in the examined pH range, in contrast to the D96N mutant (Tittor et al., 1989; Otto et al., 1989; Miller & Oesterhelt, 1990). After addition of azide, M decay is only sligthly accelerated, also in contrast to D96N. In the presence of azide, a moderate pH dependency is observed, with an increase in the M decay time with increasing pH.

Unlike D96 mutants, all surface mutants show only a small wild-type-like acceleration of the M decay time after addition of azide. This little pH-dependent effect of azide suggests that HN_3 is the species involved in the rate-limiting step, in agreement with a previous study (Tittor et al., 1994).

Time-Resolved FT-IR Spectroscopy. In time-resolved UV/Vis measurements, mutations at position 38 show the most pronounced kinetic changes in the second part of the BR photocycle (Figure 3, Table 1). For a more detailed analysis, time-resolved FT-IR difference spectroscopy was performed. Figure 5 compares step-scan measurements of BR wild type (A) with those of the point mutant D38R (B). In wild-type

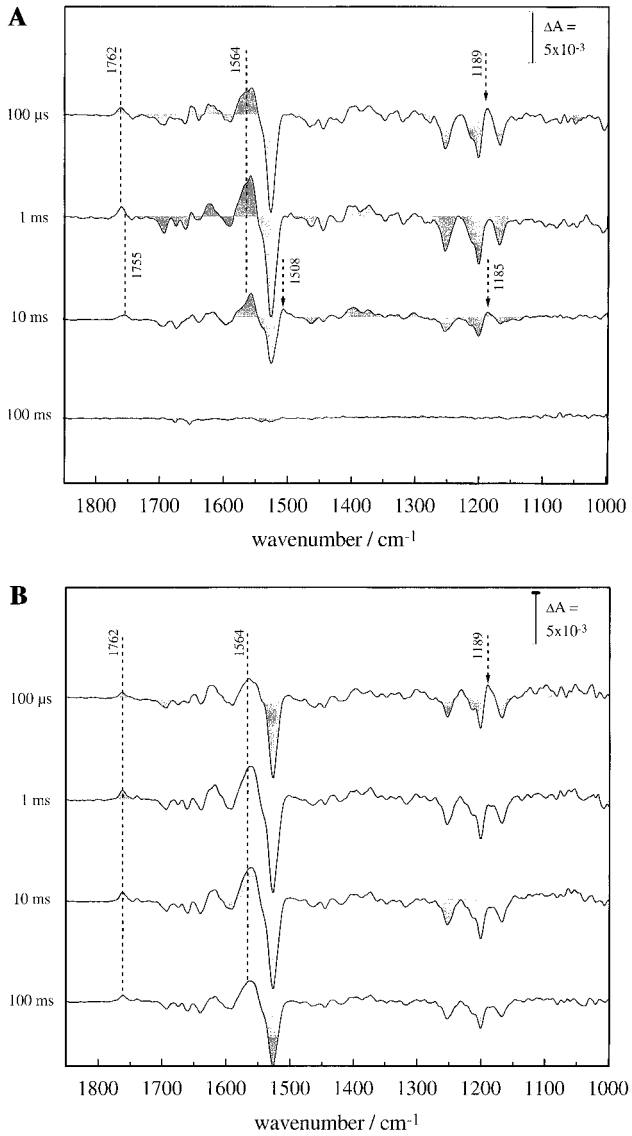

FIGURE 5: Step-scan FT-IR difference spectra of BR. Negative absorbance changes correspond to the ground state of BR. Positive bands reflect changes in vibrational modes of BR photoproducts at indicated times. (A) Wild-type BR. (B) D38R mutant.

BR, the photocycle is completed after 100 ms, resulting in an essentially flat line at that time. The flat line also demonstrates the high fidelity of the difference spectra obtained. Absorbance changes down to 10^{-4} can be reliably recorded. Up to 1 ms, difference spectra of the D38R mutant are identical to the wild-type protein, indicating that the mutation does not influence at all the properties of the mutant BR in this time regime.[2] Small differences between the spectra arise primarily from the fact that the rise of the M intermediate is slightly slower in the D38R mutant compared to the wild type (Table 1). It is not the intention of this study to assign all difference bands to specific vibrations of the protein; for this purpose, the reader is referred to the vast literature, e.g., Bagley et al. (1982), Engelhard et al. (1985), Braiman et al. (1988), Gerwert et al. (1990), Maeda et al. (1991), Pfefferlé et al. (1991), Bousché et al. (1992),

[2] At wavenumbers below 1150 cm^{-1}, the base line is slightly negative for wild-type BR and positive for the mutant. Whether this is due to measurement artifacts or to a significant change in the continuum band absorbing also at these wavenumbers has to be clarified in further studies.

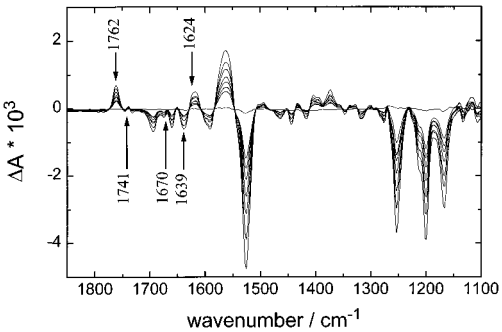

FIGURE 6: Time-resolved FT-IR spectra of the D38R mutant recorded with the rapid-scan technique. Spectra shown correspond to absorbance changes of 18, 85, 152, 219, 286, 353, 420, and 1024 ms (with decreasing amplitude) after light excitation. 1000 subsequent measurements were averaged.

Hessling et al. (1993), Weidlich & Siebert (1993), and Sasaki et al. (1994). Nevertheless, some well-characterized vibrations are briefly mentioned which are marker bands for particular photocycle intermediates; 100 μs after initiation of the photocycle, a positive difference band at 1189 cm^{-1} (C−C stretch of retinal) indicates that some BR molecules are still in the L state. The occurrence of positive bands at 1762 cm^{-1} (C═O stretch of protonated Asp85) and 1564 cm^{-1} (C═C stretch of retinal with minor contributions of the amide II band) shows the appearance of the M intermediate. These bands are more prominent at 1 ms where the maximum of M is reached. Substantial differences between wild type and the mutant D38R occur after 1 ms. The wild-type protein relaxes back to the ground state via the N and the O intermediate under the conditions applied. Among others, characteristic frequencies are the positive C═C stretch at 1508 cm^{-1} for the O intermediate, the positive C−C stretch at 1185 cm^{-1}, and the downshift of the C═O stretch of Asp85 to 1755 cm^{-1} for the N state. In the D38R mutant, none of these features appear (Figure 5B). Figure 6 shows this even more clearly. Spectra are recorded every 67 ms after the laser pulse. Due to the lower time resolution of the rapid-scan method, only difference spectra starting with the M intermediate are recorded. For example, the pair of difference bands at 1639/1624 cm^{-1} has been assigned to the vibration of the deprotonated retinal Schiff base (Aton et al., 1977; Bagley et al., 1982). Except for M, no significant accumulation of other intermediates is observed. Moreover, the difference band at 1670 cm^{-1} commonly attributed to a large conformational change of the protein moiety (Braiman et al., 1987; Gerwert et al., 1990) is almost absent in the mutant. The negative band around 1741 cm^{-1} characteristic for the deprotonation/protonation reaction of D96 is also lacking. The frequency of the carbonyl stretch of D85 remains at 1762 cm^{-1} when the mutant relaxes to the ground state. A frequency shift of this band as in wild-type BR is not detectable.

To stress this more clearly, Figure 7 depicts the temporal behavior of the above-mentioned difference bands. In addition, the C═C stretch of the ground state of BR is represented by the time trace at 1527 cm^{-1}. The traces for 1564 cm^{-1} are very similar to the kinetics detected at 412 nm (Figures 2 and 3), confirming the assignment of this band to the M intermediate; 1186 cm^{-1} is a distinct frequency where the temporal behavior of the L as well as the N intermediate is easily detected, which is hardly achieved by UV/Vis spectroscopy. Decay of L is not influenced by

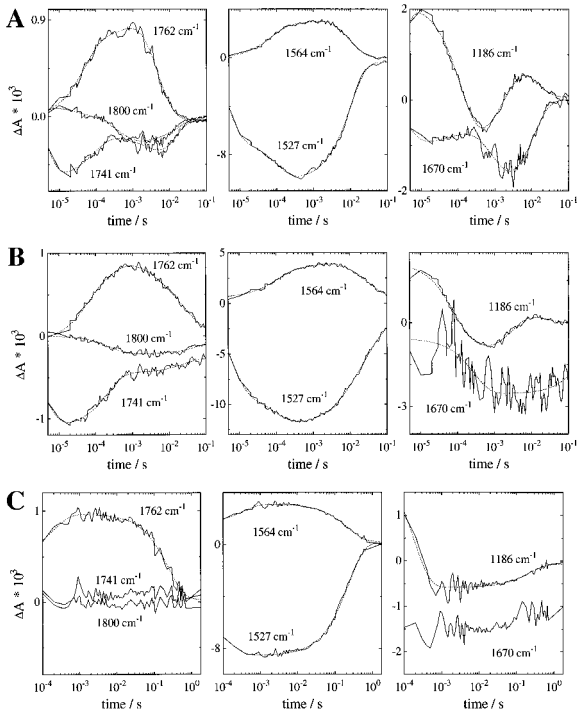

FIGURE 7: Temporal behavior of selected bands (in cm^{-1}) of (A) wild-type BR, (B) D38C mutant, and (C) D38R mutant. Note the different time scale for the measurements of D38R (C). For clarity, time traces of the absorbance changes at 1186 cm^{-1} are slightly offset. Assignment of the bands: C═O stretching vibration of Asp85 at 1762 cm^{-1}, C═O stretching vibration of Asp96 at 1741 cm^{-1}, continuum band characteristic for proton polarizability at 1800 cm^{-1}, C═C stretch of retinal in the M state at 1564 cm^{-1}, C═C stretch of retinal in the ground state of BR at 1527 cm^{-1}, C_{10}−C_{11} stretch of retinal at 1186 cm^{-1}, C═O stretch of the protein backbone (amide I) at 1670 cm^{-1}.

mutations at position 38, but the amount of N formation is less in D38C (Figure 7B) than in wild-type (Figure 7A). Moreover, N is not accumulated at all in D38R (Figure 7C).[3]

A negative difference band appears at 1670 cm^{-1} with the same time constant as N rises in wild-type BR (Figure 7A). Going from wild type via D38C to D38R, this large change disappears. This band is attributed to a conformational change of the protein leading to changes in the amide I vibration. The detailed time course confirms the conclusions drawn from the rapid-scan measurement (Figure 6).

Concomitantly with the M rise, Asp85 is protonated, as monitored by the appearance of the C═O stretch at 1762 cm^{-1}. The kinetics of this proton transfer reaction are not influenced by the mutations. Deprotonation of Asp85 is slowed down in the same order as the mutation affects M decay. Asp96, which is protonated in the ground state of BR, experiences a change in its immediate vicinity during the lifetime of L (maximum of L is reached after 20 μs), leading to a transient decrease in absorbance at 1741 cm^{-1} (Gerwert et al., 1989). This environmental change relaxes when the M intermediate is formed. During M decay, Asp96 deprotonates (second transient decrease in absorbance at 1741 cm^{-1} in Figure 7A) and gets reprotonated during N decay (compare with trace at 1186 cm^{-1} in Figure 7A for wild-type BR). The environmental change in the vicinity of

[3] The time trace for the D38C mutant at 1670 cm^{-1} is much noisier than those of the measurements with wild type and the D38R mutant. This is due to the higher water content in this sample.

Asp96 is also observed in the mutant D38C and, although less time-resolved, in the measurement of D38R (1741 cm^{-1} in Figure 7C, but note the different time scale!). The extent of transient deprotonation/reprotonation of Asp96 is less in D38C and not detectable at all in D38R.

At wavenumbers above 1770 cm^{-1}, vibrations due to the polypeptide are absent. Nevertheless, small differences occur which are attributed to a broad continuum band arising from highly polarizable protons within a hydrogen-bonded network (Eckert & Zundel, 1988; Olejnik et al., 1992; le Coutre et al., 1995). Transient absorbance changes at 1800 cm^{-1} are representative of the temporal behavior of this continuum band. In wild-type BR, a positive difference band appears during the lifetime of L. During the lifetime of N, a transient negative absorbance change is observed. As shown in Figure 7A, the kinetics for this band are the same within experimental error as the kinetics for the conformational change (1670 cm^{-1}) and for the Asp96 deprotonation/reprotonation reaction (1741 cm^{-1}). Strikingly again, the transient negative continuum band is less in D38C (1800 cm^{-1} in Figure 7B) and absent in D38R (Figure 7C).

DISCUSSION

Although there exists a fairly good picture of the spatial arrangement of those amino acid residues forming the seven membrane-spanning α-helices in bacteriorhodopsin (Henderson et al., 1990), the assignment of surface-exposed amino acids, their orientation, and especially their functional relevance for the pumping mechanism are at present mostly obscure.

To date, predominantly interior amino acid residues have been examined for their contribution to the light-energized proton pumping mechanism. The carboxyl groups of D85 and D96 have been identified as key elements of the proton release and Schiff base reprotonation reactions, respectively. However, it can be expected that particular amino acid residues of the polypeptide loops exposed to the aqueous phase, especially those at the CP membrane surface, are required for optimal vectorial proton transport across BR. During the second half of the photocycle, protons from the (under physiological conditions) alkaline aqueous phase have to be attracted by the CP membrane surface and efficiently guided to the entrance of the inwardly directed proton pathway, a hydrogen-bonded network of amino acids, water molecules, and the Schiff base (Dencher et al., 1992). The fast transient protonation dynamics of carboxylic groups, especially if they form a cluster as observed at the CP surface of BR (Nachliel et al., 1996), make aspartic and glutamic acids suitable elements for efficient collection and fast transfer of protons from the medium to the CP proton pathway. The amino acid residue at the entrance of this pathway has to fulfill a dual function: interaction with the proton-collecting amino acids at the surface to attract the proton and interaction with the elements of the hydrogen-bonded network to allow efficient proton transfer along this path.

To identify those amino acids at the CP protein surface involved in these elementary proton transfer reaction steps, the aspartic and glutamic amino acids D36, D38, D102, D104, and E161 (Figure 1) were replaced by cysteine and arginine residues, and the effect of these replacements on the photocycle and pumping cycle was examined. The light-triggered proton transfer reactions from the EC membrane surface into the aqueous medium and to the CP surface were probed with the optical pH-sensor pyranine residing in the aqueous bulk medium by applying time-resolved visible absorption spectroscopy. Since the proton transfer processes inside the protein are reflected in the kinetics of the photocycle intermediates, a correlation with the external proton transfer reactions is feasible. On the other hand, our data could only be understood at the molecular level by time-resolved FT-IR spectroscopy.

Of the five cytoplasmic amino acids studied, only the replacement of D38 by cysteine or arginine, i.e., of a negatively charged residue by a neutral or positive one (at the pH of the investigation), resulted in severe alterations of the reaction steps inside BR during the second half of the photocycle. As illustrated in Figures 5−7 for the mutant D38R, in the FT-IR spectra many features characteristic for wild-type BR are not observed in the second half of the photocycle. There are no indications for accumulation of the intermediates N and O; i.e., photoexcited BR relaxes from the M intermediate to the ground state with a rate-limiting step which does not involve N or O. In this mutant, therefore, a pure M state develops without contributions by later intermediates (Figure 6). The M−BR FT-IR difference spectrum of D38R is almost identical to the wild type reconstructed by global analysis (Souvignier & Gerwert, 1992).

However, there is no indication for a difference band due to D38 when time-resolved FT-IR spectra of wild type and of the D38 mutants are compared. In this case, the mutation should lead to an abolishment of the difference band in the carbonyl stretch region which is actually not observed. The shifting of the C═O stretch from 1762 to 1755 cm^{-1} during the M−N transition was attributed to a change in microenvironment of D85 (Braiman et al., 1991). This interpretation was challenged by resonance Raman measurements (Eisfeld et al., 1993). Indeed, in the D38R mutant, no shifting of the 1762 cm^{-1} band occurs. However, there is still a shift in D38C although less pronounced as compared to wild type. We, therefore, suggest D38 to be a silent member of the proton uptake pathway. The dwell time for a proton at D38 might be too short to be observable. This might be caused by a relatively low p*K* of this group which makes the protonation step rate-limiting and the trigger for the faster subsequent events. Furthermore, alterations in vibrational bands indicative of large conformational changes in the protein moiety (monitored at 1670 cm^{-1} in Figure 7) and of the transient deprotonation/reprotonation of D96 (1741 cm^{-1}) occurring in the wild type during N formation are absent in D38R. At present, it is not known if in the mutant D38R these features are only kinetically invisible or really absent. In the mutant D38C, all these features are much less pronounced than in wild-type BR. Surprisingly, and not observed for any of the previously studied mutants, although conformational changes and transient deprotonation of D96 and the intermediates N are O are not observed—reactions assumed to be inherently involved in vectorial proton transfer across BR—D38R is still a functional proton pump. Light-induced proton release (as detected by pyranine) is not affected, and although there is a pronounced "kinetic defect" in proton uptake (Figure 3, Table 1), the proton pumping capability of D38C and D38R cells is still 55% and 30%, respectively, of the wild-type activity. In accordance with

this, mutant D38R cells can grow autotrophically, contrary to D96N. In spite of the pronounced alterations during the second half of the photocycle, the first part of the cycle leading to the M intermediate remains quite unaffected in the D38 mutants as well as in D36C and E161C. This justifies previous experiments where these residues have been labeled with optical pH sensors to probe lateral proton transfer reactions [see Heberle et al. (1994)].

Contrary to C36 and C161, which could be modified by all three maleimide dyes applied, C38 is accessible only for FMI, indicating a more buried location of D38 in BR. Only a spin-label at residue 38, but not at C36 and C161, has a comparatively decreased mobility (T. Rink and H.-J. Steinhoff, unpublished results). Furthermore, the temporal relationship of M decay kinetics and proton uptake differs considerably between the various amino acid residues examined. Whereas in the mutants D36C and E161C proton uptake proceeds slower than the main component of M decay and the monoexponentially fitted M decay, in D38C and D38R both processes occur simultaneously (Table 1). This suggests that for mutated D38 the reprotonation of the deprotonated Schiff base from the hydrogen-bonded network becomes the rate-limiting step, but not proton uptake to the CP surface as in D36C and E161C. Therefore, contrary to the two latter amino acids and possibly D102 and D104 too, which seem to be freely surface-exposed and employed in attracting protons from the aqueous bulk phase, D38 directly belongs to the internal reprotonation pathway. It is also remarkable that although in the mutant $D_2102,104R_2$ two negatively charged residues are replaced by two positively charged residues, the retardation of M decay and proton uptake is stronger in D38R, again indicating the particular properties of this residue for the pumping mechanism. The observation by FT-IR spectroscopy that replacement of D38 reduces the extent of the light-induced conformational changes in the protein moiety and the transient deprotonation of D96 is additional evidence for the participation of residue D38 in the CP proton pathway. The modulation of the broad IR continuum band (probed at 1800 cm^{-1} in Figure 7), which arises from highly polarizable protons within a hydrogen-bonded network (Olejnik et al., 1992), in response to the charge of residue 38, can be considered as proof for the direct participation of this residue in the CP proton uptake pathway. The transient negative continuum band developing in wild-type BR during N formation, concomitant with the conformational changes and deprotonation of D96, is less pronounced in mutant D38C and absent in D38R. A similar impairment of the temporal behavior of the continuum band is observed for the D96N replacement (le Coutre et al., 1995), placing D38 and D96 in the same tightly coupled hydrogen-bonded network creating the CP reprotonation pathway.

This hydrogen-bonded network, gated by conformational changes in the protein moiety at the CP side of the Schiff base linkage, seems to extend from the CP surface at least to D85, since feedback between D85 and the proton uptake pathway was demonstrated (Heberle et al., 1993). Also, changes in the chemical environment of D96 are occurring already in the L intermediate (Gerwert et al., 1989). In addition, the rise time of the M intermediate, representing proton transfer from the Schiff base to Asp85, is decelerated by a factor of 2−3 when amino acids participating in the proton uptake reaction are exchanged, as in D38R, $D_2102,-104R_2$ (Table 1), or D96N (J. Heberle, unpublished results). A similar long-range effect was recently found for proton transfer in the bacterial photosyntetic reaction center (Maróti et al., 1995).

The overall photocycling time of D38R approaches values similar to D96 mutants (Miller & Oesterhelt, 1990). It is worth comparing the effect of both mutations more thoroughly. Exchange of D96 by a nonprotonatable residue leads to drastic pH dependence of the late photocycle intermediates (Tittor et al., 1989; Otto et al., 1989; Miller & Oesterhelt, 1990). The "kinetic deficiency" can be overcome by addition of azide (Tittor et al., 1989). Figure 4 demonstrates that M decay of D38R neither depends significantly on pH nor does the presence of 0.5 M azide accelerate M decay in the same way as it does in D96 mutants. From the temperature dependence of the M decay rate of the D38 mutants, activation enthalpies and entropies have been calculated (data not shown). They are in the range of the values for wild-type BR. Contrary to this, D96 mutants exhibit low activation enthalpies, and the M decay is mainly entropically driven (Miller & Oesterhelt, 1990). As stated above, D38R relaxes from the M intermediate directly to the ground state. Yet in the D96N mutant, later intermediates have been detected [M_N and N (Sasaki et al., 1992; Eisfeld, 1994)]. All these data show that the role of D38 is quite different from D96. From the structural data available (cf. Figure 1), D38 would be a good candidate for reprotonation of D96. Thus, mutating D38 should result in accumulation of the N intermediate. However, a pure M intermediate is formed. From these findings, we suggest that D38 plays an important role in the conformational change of the protein. Changes in tertiary structure during the photocycle have been elucidated close to helices F and G, and also at helix B where D38 is located (Dencher et al., 1989; Koch et al., 1991; Subramaniam et al., 1993). The conformational change of BR might transiently decrease the p*K* of D96, leading to the reprotonation of the Schiff base. In D38R, and to a lesser extent in D38C, this conformational change is delayed. Consequently, D96 is not able to donate the proton to the Schiff base, thereby prolonging M decay (Figure 3). This is consistent with the results of FT-IR spectroscopy (Figures 6 and 7) that in D38R no difference band due to the carbonyl stretching of D96 is observable. For simple kinetic reasons, the amide I difference band at 1670 cm^{-1} cannot accumulate because in D38R the resetting of the conformational change is faster than its formation.

It could be demonstrated that amino acids located at the surface of a protein are of functional importance. Replacing D38 in BR, which is approximately 12 Å apart from the retinal Schiff base, by R slows down M decay by a factor of 20. D38 is not only of importance for channelling protons from the CP surface of the purple membrane to the active center of BR, but is also a requirement for the temporal optimal occurrence of light-induced conformational changes of the protein and of the transient deprotonation of D96. Surprisingly, the D38-deficient proton pump is still functional and only kinetically impaired.

ACKNOWLEDGMENT

We thank Dr. J. Tittor for critical comments on parts of the manuscript, Dr. J. Rudolph for improving the English style, and C. Zscherp for help in data processing. J.H. is indebted to Dr. G. Büldt to continuous support.

REFERENCES

Alexiev, U., Mollaaghababa, R., Scherrer, P., Khorana, H. G., & Heyn, M. P. (1995) *Proc. Natl. Acad. Sci. U.S.A. 92*, 372−376.

Aton, B., Doukas, A. G., Callender, R. H., Becher, B., & Ebrey, T. G. (1977) *Biochemistry 16*, 2995−2999.

Bagley, K., Dollinger, G., Eisenstein, L., Singh, A. K., & Zimányi, L. (1982) *Proc. Natl. Acad. Sci. U.S.A. 79*, 4972−4976.

Blaurock, A. E., & Stoeckenius, W. (1971) *Nature (London), New Biol. 233*, 10−16.

Bousché, O., Sonar, S., Krebs, M. P., Khorana, H. G., & Rothschild, K. J. (1992) *Photochem. Photobiol. 56*, 1085−1095.

Boyer, P. D., Chance, B., Ernster, P., Mitchell, E., Racker, E., & Slater, E. C. (1977) *Annu. Rev. Biochem. 46*, 955−1026.

Braiman, M. S., Ahl, P. L., & Rothschild, K. J. (1987) *Proc. Natl. Acad. Sci. U.S.A. 84*, 5221−5225.

Braiman, M. S., Mogi, T., Marti, T., Stern, L. J., Khorana, H. G., & Rothschild, K. J. (1988) *Biochemistry 27*, 8516−8520.

Braiman, M. S., Bousché, O., & Rothschild, K. J. (1991) *Proc. Natl. Acad. Sci. U.S.A. 88*, 2388−2392.

Burghaus, P. A., & Dencher, N. A. (1989) *Arch. Biochem. Biophys. 275*, 395−409.

Butt, H. J., Fendler, K., Bamberg, E., Tittor, J., & Oesterhelt, D. (1989) *EMBO J. 8*, 1657−1663.

Cao, Y., Brown, L. S., Needleman, R., & Lanyi, J. K. (1993) *Biochemistry 32*, 10239−10248.

Dencher, N. A., Dresselhaus, D., Zaccai, G., & Büldt, G. (1989) *Proc. Natl. Acad. Sci. U.S.A. 86*, 7876−7879.

Dencher, N. A., Heberle, J., Büldt, G., Höltje, H.-D., & Höltje, M. (1992) in *Membrane proteins*: *stuctures, interactions and models* (Pullman, A., et al., Eds.) pp 69−84, Kluwer Academic Publishers, Dordrecht, The Netherlands.

Eckert, M., & Zundel, G. (1988) *J. Phys. Chem. 92*, 7016−7023.

Eisfeld, W. (1994) Ph.D. Thesis, Göttingen.

Eisfeld, W., Pusch, C., Diller, R., Lohrmann, R., & Stockburger, M. (1993) *Biochemistry 32*, 7196−7215.

Engelhard, M., Gerwert, K., Hess, B., & Siebert, F. (1985) *Biochemistry 24*, 400−407.

Engelhard, M., Pevec, B., & Hess, B. (1989) *Biochemistry 28*, 5432−5438.

Engelhard, M., Kohl, K. D., Mueller, K. H., Hess, B., Heidemeier, J., Fischer, M., & Parak, F. (1990) *Eur. Biophys. J. 19*, 11−18.

Ferrando, E., Schweiger, U., & Oesterhelt, D. (1993) *Gene 125*, 41−47.

Gerwert, K., Hess, B., Soppa, J., & Oesterhelt, D. (1989) *Proc. Natl. Acad. Sci. U.S.A. 86*, 4943−4947.

Gerwert, K., Souvignier, G., & Hess, B. (1990) *Proc. Natl. Acad. Sci. U.S.A. 87*, 9774−9778.

Grzesiek, S., & Dencher, N. A. (1986) *FEBS Lett. 208*, 337−342.

Heberle, J., & Dencher, N. A. (1990) *FEBS Lett. 277*, 277−280.

Heberle, J., & Dencher, N. A. (1992a) *Proc. Natl. Acad. Sci. U.S.A. 89*, 5996−6000.

Heberle, J., & Dencher, N. A. (1992b) in *Proton Transfer in Hydrogen-Bonded Systems* (Bountis, T., Ed.) pp 187−197, Plenum Press, New York.

Heberle, J., & Zscherp, C. (1996) *Appl. Spectrosc. 50* (in press).

Heberle, J., Oesterhelt, D., & Dencher, N. A. (1993) *EMBO J. 12*, 3721−3727.

Heberle, J., Riesle, J., Thiedemann, G., Oesterhelt, D., & Dencher, N. A. (1994) *Nature 370*, 379−382.

Henderson, R., Baldwin, J. M., Ceska, T. A., Zemlin, F., Beckmann, E., & Downing, K. H. (1990) *J. Mol. Biol. 213*, 899−929.

Hessling, B., Souvignier, G., & Gerwert, K. (1993) *Biophys. J. 65*, 1929−1941.

Koch, M. H. J., Dencher, N. A., Oesterhelt, D., Plöhn, H.-J., Rapp, G., & Büldt, G. (1991) *EMBO J. 10*, 521−526.

Kraulis, P. (1991) *J. Appl. Crystallogr. 24*, 946−950.

Lanyi, J. K. (1993) *Biochim. Biophys. Acta 1183*, 241−261.

le Coutre, J., Tittor, J., Oesterhelt, D., & Gerwert, K. (1995) *Proc. Natl. Acad. Sci. U.S.A. 92*, 4962−4966.

Maeda, A., Sasaki, J., Pfefferlé, J.-M., Shichida, Y., & Yoshizawa, T. (1991) *Photochem. Photobiol. 54*, 911−921.

Maróti, P., Hanson, D. K., Schiffer, M., & Sebban, P. (1995) *Nat. Struct. Biol. 12*, 1057−1059.

Miller, A., & Oesterhelt, D. (1990) *Biochim. Biophys. Acta 1020*, 57−64.

Mitchell, P. (1961) *Nature 191*, 144−148.

Mogi, T., Stern, L. J., Marti, T., Chao, B. H., & Khorana, H. G. (1988) *Proc. Natl. Acad. Sci. U.S.A. 85*, 4148−4152.

Nachliel, E., Gutman, E., Kiryati, M., & Dencher, N. A. (1996) *Proc. Natl. Acad. Sci. U.S.A. 93* (in press).

Oesterhelt, D. (1982) *Methods Enzymol. 88*, 10−17.

Oesterhelt, D., & Stoeckenius, W. (1971) *Nature (London), New Biol. 233*, 149−152.

Oesterhelt, D., & Stoeckenius, W. (1974) *Methods Enzymol. 31*, 667−686.

Oesterhelt, D., Tittor, J., & Bamberg, E. (1992) *J. Bioenerg. Biomembr. 24*, 181−191.

Olejnik, J., Brzezinsky, B., & Zundel, G. (1992) *J. Mol. Struct. 271*, 157−173.

Otto, H., Marti, T., Holz, M., Mogi, T., Lindau, M., Khorana, H. G., & Heyn, M. P. (1989) *Proc. Natl. Acad. Sci. U.S.A. 86*, 9228−9232.

Pfefferlé, J.-M., Maeda, A., Sasaki, J., & Yoshizawa, T. (1991) *Biochemistry 30*, 6548−6556.

Sasaki, J., Shichida, Y., Lanyi, J. K., & Maeda, A. (1992) *J. Biol. Chem. 267*, 20782−20786.

Sasaki, J., Lanyi, J. K., Needleman, R., Yoshizawa, T., & Maeda, A. (1994) *Biochemistry 33*, 3178−3184.

Souvignier, G., & Gerwert, K. (1992) *Biophys. J. 63*, 1393−1405.

Stern, L. J., Ahl, P. L., Marti, T., Mogi, T., Dunach, M., Berkowitz, S., Rothschild, & K. J., Khorana, H. G. (1989) *Biochemistry 28*, 10035−10042.

Subramaniam, S., Gerstein, M., Oesterhelt, D., & Henderson, R. (1993) *EMBO J. 12*, 1−8.

Tittor, J., Soell, C., Oesterhelt, D., Butt, H.-J., & Bamberg, E. (1989) *EMBO J. 8*, 3477−3482.

Tittor, J., Wahl, M., Schweiger, U., & Oesterhelt, D. (1994) *Biochim. Biophys. Acta 1187*, 191−197.

Wagner, G., Oesterhelt, D., Krippahl, G., & Lanyi, J. K. (1981) *FEBS Lett. 131*, 341−345.

Weidlich, O., & Siebert, F. (1993) *Appl. Spectrosc. 47*, 1394−1400.

BI9600456